Search for heavy particles decaying into electron-positron pairs in $p\bar{p}$ collisions

The DØ Collaboration *
Fermi National Accelerator Laboratory, Batavia, Illinois 60510

(June 29, 2000)

Abstract

We present preliminary results of searches for technirho (ρ_T), techniomega (ω_T), and Z' particles, using the decay channels $\rho_T, \omega_T, Z' \to e^+e^-$. The search is based on 120.9 pb^{-1} of data collected by the DØ detector at the Tevatron during 1992-1996. In the absence of a signal, we set 95% CL upper limits on the cross sections for the processes $\rho_T, \omega_T \to e^+e^-$ and $Z' \to e^+e^-$ as a function of the mass of the decaying particle. For certain model parameters, we exclude the existence of degenerate ρ_T and ω_T states with masses below 207 GeV. We exclude a Z' with mass below 670 GeV, assuming that it has the same couplings to fermions as the Z boson.

*Submitted to the *International Conference on High Energy Physics,* July 27 – August 2, 2000, Osaka, Japan.

B. Abbott,[48] M. Abolins,[45] V. Abramov,[21] B.S. Acharya,[15] D.L. Adams,[55] M. Adams,[32] G.A. Alves,[2] N. Amos,[44] E.W. Anderson,[37] M.M. Baarmand,[50] V.V. Babintsev,[21] L. Babukhadia,[50] A. Baden,[41] B. Baldin,[31] S. Banerjee,[15] J. Bantly,[54] E. Barberis,[24] P. Baringer,[38] J.F. Bartlett,[31] U. Bassler,[11] A. Bean,[38] M. Begel,[49] A. Belyaev,[20] S.B. Beri,[13] G. Bernardi,[11] I. Bertram,[22] A. Besson,[9] V.A. Bezzubov,[21] P.C. Bhat,[31] V. Bhatnagar,[13] M. Bhattacharjee,[50] G. Blazey,[33] S. Blessing,[29] A. Boehnlein,[31] N.I. Bojko,[21] F. Borcherding,[31] A. Brandt,[55] R. Breedon,[25] G. Briskin,[54] R. Brock,[45] G. Brooijmans,[31] A. Bross,[31] D. Buchholz,[34] M. Buehler,[32] V. Buescher,[49] V.S. Burtovoi,[21] J.M. Butler,[42] F. Canelli,[49] W. Carvalho,[3] D. Casey,[45] Z. Casilum,[50] H. Castilla-Valdez,[17] D. Chakraborty,[50] K.M. Chan,[49] S.V. Chekulaev,[21] D.K. Cho,[49] S. Choi,[28] S. Chopra,[51] B.C. Choudhary,[28] J.H. Christenson,[31] M. Chung,[32] D. Claes,[46] A.R. Clark,[24] J. Cochran,[28] L. Coney,[36] B. Connolly,[29] W.E. Cooper,[31] D. Coppage,[38] M.A.C. Cummings,[33] D. Cutts,[54] O.I. Dahl,[24] G.A. Davis,[49] K. Davis,[23] K. De,[55] K. Del Signore,[44] M. Demarteau,[31] P. Demine,[9] D. Denisov,[31] S.P. Denisov,[21] H.T. Diehl,[31] M. Diesburg,[31] G. Di Loreto,[45] S. Doulas,[43] P. Draper,[55] Y. Ducros,[12] L.V. Dudko,[20] S.R. Dugad,[15] A. Dyshkant,[21] D. Edmunds,[45] J. Ellison,[28] V.D. Elvira,[31] R. Engelmann,[50] S. Eno,[41] G. Eppley,[57] P. Ermolov,[20] O.V. Eroshin,[21] J. Estrada,[49] H. Evans,[47] V.N. Evdokimov,[21] T. Fahland,[27] S. Feher,[31] D. Fein,[23] T. Ferbel,[49] H.E. Fisk,[31] Y. Fisyak,[51] E. Flattum,[31] F. Fleuret,[24] M. Fortner,[33] K.C. Frame,[45] S. Fuess,[31] E. Gallas,[31] A.N. Galyaev,[21] P. Gartung,[28] V. Gavrilov,[19] R.J. Genik II,[22] K. Genser,[31] C.E. Gerber,[31] Y. Gershtein,[54] B. Gibbard,[51] R. Gilmartin,[29] G. Ginther,[49] B. Gómez,[5] G. Gómez,[41] P.I. Goncharov,[21] J.L. González Solís,[17] H. Gordon,[51] L.T. Goss,[56] K. Gounder,[28] A. Goussiou,[50] N. Graf,[51] P.D. Grannis,[50] J.A. Green,[37] H. Greenlee,[31] S. Grinstein,[1] P. Grudberg,[24] S. Grünendahl,[31] A. Gupta,[15] S.N. Gurzhiev,[21] G. Gutierrez,[31] P. Gutierrez,[53] N.J. Hadley,[41] H. Haggerty,[31] S. Hagopian,[29] V. Hagopian,[29] K.S. Hahn,[49] R.E. Hall,[26] P. Hanlet,[43] S. Hansen,[31] J.M. Hauptman,[37] C. Hays,[47] C. Hebert,[38] D. Hedin,[33] A.P. Heinson,[28] U. Heintz,[42] T. Heuring,[29] R. Hirosky,[32] J.D. Hobbs,[50] B. Hoeneisen,[8] J.S. Hoftun,[54] A.S. Ito,[31] S.A. Jerger,[45] R. Jesik,[35] K. Johns,[23] M. Johnson,[31] A. Jonckheere,[31] M. Jones,[30] H. Jöstlein,[31] A. Juste,[31] S. Kahn,[51] E. Kajfasz,[10] D. Karmanov,[20] D. Karmgard,[36] R. Kehoe,[36] S.K. Kim,[16] B. Klima,[31] C. Klopfenstein,[25] B. Knuteson,[24] W. Ko,[25] J.M. Kohli,[13] A.V. Kostritskiy,[21] J. Kotcher,[51] A.V. Kotwal,[47] A.V. Kozelov,[21] E.A. Kozlovsky,[21] J. Krane,[37] M.R. Krishnaswamy,[15] S. Krzywdzinski,[31] M. Kubantsev,[39] S. Kuleshov,[19] Y. Kulik,[50] S. Kunori,[41] V. Kuznetsov,[28] G. Landsberg,[54] A. Leflat,[20] F. Lehner,[31] J. Li,[55] Q.Z. Li,[31] J.G.R. Lima,[3] D. Lincoln,[31] S.L. Linn,[29] J. Linnemann,[45] R. Lipton,[31] A. Lucotte,[50] L. Lueking,[31] C. Lundstedt,[46] A.K.A. Maciel,[33] R.J. Madaras,[24] V. Manankov,[20] S. Mani,[25] H.S. Mao,[4] T. Marshall,[35] M.I. Martin,[31] R.D. Martin,[32] K.M. Mauritz,[37] B. May,[34] A.A. Mayorov,[35] R. McCarthy,[50] J. McDonald,[29] T. McMahon,[52] H.L. Melanson,[31] X.C. Meng,[4] M. Merkin,[20] K.W. Merritt,[31] C. Miao,[54] H. Miettinen,[57] D. Mihalcea,[53] A. Mincer,[48] C.S. Mishra,[31] N. Mokhov,[31] N.K. Mondal,[15] H.E. Montgomery,[31] M. Mostafa,[1] H. da Motta,[2] E. Nagy,[10] F. Nang,[23] M. Narain,[42] V.S. Narasimham,[15] H.A. Neal,[44] J.P. Negret,[5] S. Negroni,[10] D. Norman,[56] L. Oesch,[44] V. Oguri,[3] B. Olivier,[11] N. Oshima,[31] P. Padley,[57] L.J. Pan,[34] A. Para,[31] N. Parashar,[43] R. Partridge,[54] N. Parua,[9] M. Paterno,[49] A. Patwa,[50] B. Pawlik,[18] J. Perkins,[55] M. Peters,[30] R. Piegaia,[1] H. Piekarz,[29] B.G. Pope,[45] E. Popkov,[36] H.B. Prosper,[29] S. Protopopescu,[51] J. Qian,[44] P.Z. Quintas,[31]

R. Raja,[31] S. Rajagopalan,[51] E. Ramberg,[31] N.W. Reay,[39] S. Reucroft,[43] J. Rha,[28]
M. Rijssenbeek,[50] T. Rockwell,[45] M. Roco,[31] P. Rubinov,[31] R. Ruchti,[36] J. Rutherfoord,[23]
A. Santoro,[2] L. Sawyer,[40] R.D. Schamberger,[50] H. Schellman,[34] A. Schwartzman,[1]
J. Sculli,[48] N. Sen,[57] E. Shabalina,[20] H.C. Shankar,[15] R.K. Shivpuri,[14] D. Shpakov,[50]
M. Shupe,[23] R.A. Sidwell,[39] V. Simak,[7] H. Singh,[28] J.B. Singh,[13] V. Sirotenko,[33]
P. Slattery,[49] E. Smith,[53] R.P. Smith,[31] R. Snihur,[34] G.R. Snow,[46] J. Snow,[52] S. Snyder,[51]
J. Solomon,[32] V. Sorín,[1] M. Sosebee,[55] N. Sotnikova,[20] K. Soustruznik,[6] M. Souza,[2]
N.R. Stanton,[39] G. Steinbrück,[47] R.W. Stephens,[55] M.L. Stevenson,[24] F. Stichelbaut,[51]
D. Stoker,[27] V. Stolin,[19] D.A. Stoyanova,[21] M. Strauss,[53] K. Streets,[48] M. Strovink,[24]
L. Stutte,[31] A. Sznajder,[3] W. Taylor,[50] S. Tentindo-Repond,[29] J. Thompson,[41]
D. Toback,[41] T.G. Trippe,[24] A.S. Turcot,[51] P.M. Tuts,[47] P. van Gemmeren,[31] V. Vaniev,[21]
R. Van Kooten,[35] N. Varelas,[32] A.A. Volkov,[21] A.P. Vorobiev,[21] H.D. Wahl,[29] H. Wang,[34]
Z.-M. Wang,[50] J. Warchol,[36] G. Watts,[58] M. Wayne,[36] H. Weerts,[45] A. White,[55]
J.T. White,[56] D. Whiteson,[24] J.A. Wightman,[37] S. Willis,[33] S.J. Wimpenny,[28]
J.V.D. Wirjawan,[56] J. Womersley,[31] D.R. Wood,[43] R. Yamada,[31] P. Yamin,[51] T. Yasuda,[31]
K. Yip,[31] S. Youssef,[29] J. Yu,[31] Z. Yu,[34] M. Zanabria,[5] H. Zheng,[36] Z. Zhou,[37] Z.H. Zhu,[49]
M. Zielinski,[49] D. Zieminska,[35] A. Zieminski,[35] V. Zutshi,[49] E.G. Zverev,[20]
and A. Zylberstejn[12]

(DØ Collaboration)

[1]Universidad de Buenos Aires, Buenos Aires, Argentina
[2]LAFEX, Centro Brasileiro de Pesquisas Físicas, Rio de Janeiro, Brazil
[3]Universidade do Estado do Rio de Janeiro, Rio de Janeiro, Brazil
[4]Institute of High Energy Physics, Beijing, People's Republic of China
[5]Universidad de los Andes, Bogotá, Colombia
[6]Charles University, Prague, Czech Republic
[7]Institute of Physics, Academy of Sciences, Prague, Czech Republic
[8]Universidad San Francisco de Quito, Quito, Ecuador
[9]Institut des Sciences Nucléaires, IN2P3-CNRS, Universite de Grenoble 1, Grenoble, France
[10]CPPM, IN2P3-CNRS, Université de la Méditerranée, Marseille, France
[11]LPNHE, Universités Paris VI and VII, IN2P3-CNRS, Paris, France
[12]DAPNIA/Service de Physique des Particules, CEA, Saclay, France
[13]Panjab University, Chandigarh, India
[14]Delhi University, Delhi, India
[15]Tata Institute of Fundamental Research, Mumbai, India
[16]Seoul National University, Seoul, Korea
[17]CINVESTAV, Mexico City, Mexico
[18]Institute of Nuclear Physics, Kraków, Poland
[19]Institute for Theoretical and Experimental Physics, Moscow, Russia
[20]Moscow State University, Moscow, Russia
[21]Institute for High Energy Physics, Protvino, Russia
[22]Lancaster University, Lancaster, United Kingdom
[23]University of Arizona, Tucson, Arizona 85721
[24]Lawrence Berkeley National Laboratory and University of California, Berkeley, California 94720

[25]University of California, Davis, California 95616
[26]California State University, Fresno, California 93740
[27]University of California, Irvine, California 92697
[28]University of California, Riverside, California 92521
[29]Florida State University, Tallahassee, Florida 32306
[30]University of Hawaii, Honolulu, Hawaii 96822
[31]Fermi National Accelerator Laboratory, Batavia, Illinois 60510
[32]University of Illinois at Chicago, Chicago, Illinois 60607
[33]Northern Illinois University, DeKalb, Illinois 60115
[34]Northwestern University, Evanston, Illinois 60208
[35]Indiana University, Bloomington, Indiana 47405
[36]University of Notre Dame, Notre Dame, Indiana 46556
[37]Iowa State University, Ames, Iowa 50011
[38]University of Kansas, Lawrence, Kansas 66045
[39]Kansas State University, Manhattan, Kansas 66506
[40]Louisiana Tech University, Ruston, Louisiana 71272
[41]University of Maryland, College Park, Maryland 20742
[42]Boston University, Boston, Massachusetts 02215
[43]Northeastern University, Boston, Massachusetts 02115
[44]University of Michigan, Ann Arbor, Michigan 48109
[45]Michigan State University, East Lansing, Michigan 48824
[46]University of Nebraska, Lincoln, Nebraska 68588
[47]Columbia University, New York, New York 10027
[48]New York University, New York, New York 10003
[49]University of Rochester, Rochester, New York 14627
[50]State University of New York, Stony Brook, New York 11794
[51]Brookhaven National Laboratory, Upton, New York 11973
[52]Langston University, Langston, Oklahoma 73050
[53]University of Oklahoma, Norman, Oklahoma 73019
[54]Brown University, Providence, Rhode Island 02912
[55]University of Texas, Arlington, Texas 76019
[56]Texas A&M University, College Station, Texas 77843
[57]Rice University, Houston, Texas 77005
[58]University of Washington, Seattle, Washington 98195

I. INTRODUCTION

Historically, the decay to lepton-antilepton pairs – in particular e^+e^- and $\mu^+\mu^-$ – has been an important discovery channel for new particles. The J/ψ, Υ, and Z have all been discovered in this way. Many extensions of the standard model predict the existence of particles that decay to lepton-antilepton pairs. Examples are heavy gauge bosons (Z') and technihadrons (ρ_T, ω_T).

The lepton-antilepton signature is a preferred channel for particle searches in strong interactions because of the relatively low backgrounds compared to hadronic decay channels. Electrons and muons are relatively easy to trigger on and their momenta can be measured precisely. Thus particles that decay to e^+e^- or $\mu^+\mu^-$ can be identified as resonances in the dilepton mass spectrum.

We describe a search for resonances in the e^+e^- mass spectrum from the data collected by DØ during Run I (Ia, Ib, and Ic) of the Fermilab Tevatron. In the following, we first describe the data sample, background sources, acceptance and efficiency. We then set limits on the cross section times branching fraction for the processes $p\overline{p} \rightarrow V + X$, followed by $V \rightarrow e^+e^-$, where V is a narrow state. Finally, we compare this limit as a function of the mass of V to predictions for various hypothetical particles.

II. DATA SELECTION AND BACKGROUNDS

The data sample, background predictions, event selection and electron identification criteria used for this analysis are identical to those described in Ref. [1]. The major difference with this analysis lies in the binning of the dielectron mass spectrum, in the signal acceptance, and in the calculation of the limit.

The dielectron invariant mass spectra for events with both electrons in the central region (CC/CC) and with one electron in the central and the other in the forward region (CC/EC) are shown in figures 1 and 3. The superimposed histogram is the estimated background. For easier comparision between data and estimated background at high mass values, we also plot the integrated spectra in Figs. 2 and 4. At each x-value, the number of events with dielectron mass above x is plotted. The data correspond to an integrated luminosity of 120.9 pb$^-$1.

The background originates from two major sources:

- Drell-Yan process (via intermediate γ and Z).
- Jets misidentified as electrons. This estimate includes contributions from
  - Dijet events in which both jets are misidentified as electrons;
  - W+jets events in which one of the jets is misidentified as an electron;
  - γ+jet events in which both the jet and γ are misidentified as electrons.

Certain backgrounds ($W\gamma$, $Z\gamma$, $t\bar{t}$, WW, and $\gamma^*/Z \rightarrow \tau\tau$) that can in principle also contribute to e^+e^- final states, have not been included in this analysis. As shown in Ref.

TABLE I. K-factor for Drell-Yan background.

Mass Range	Cross Sections (mb)		K-Factor
	Pythia	Van Neerven	
60-75	6.24E-9	7.09E-9	1.14
75-105	1.74E-7	2.16E-7	1.24
105-120	2.68E-9	3.50E-9	1.31
120-160	1.52E-9	1.88E-9	1.24
160-200	3.71E-10	4.44E-10	1.20
200-250	1.60E-10	1.91E-10	1.19
250-300	6.07E-11	7.23E-11	1.19
300-350	2.62E-11	3.15E-11	1.20
350-450	1.83E-11	2.24E-11	1.22
450-1000	5.47E-12	6.89E-12	1.26

[1], these are several orders of magnitude smaller than the two main backgrounds and have therefore been ignored.

The Drell-Yan background is estimated using the PYTHIA Monte Carlo generator [2]. A K-factor is applied as a function of the dielectron mass, in order to normalize the cross sections from PYTHIA to those predicted by the next-to-leading order calculation by Van Neerven et al., as described in Ref. [1]. The K-factors used for different mass regions are listed in Table I. We use an uncertainty of 3% for the K factor. Figures 5 and 6 show the total background and the two separate components for the CC/CC and CC/EC events, after taking the K-factor into account.

III. ACCEPTANCE

The acceptance for a ρ_T or $\omega_T \to e^+e^-$ signal as a function of the mass of the ρ_T or ω_T (we assume them to have equal masses), is tabulated in Table II and plotted in Fig. 7. The efficiency for observing a signal at a given mass, after accounting for the dielectron identification efficiency in different detector regions, is plotted in Fig. 8. The dielectron efficiencies as taken from Ref. [1] are

$$\begin{aligned} \epsilon_{ee} &= 0.814 \pm 0.014 \text{ for CC/CC events} \\ \epsilon_{ee} &= 0.479 \pm 0.010 \text{ for CC/EC events.} \end{aligned} \tag{1}$$

The expected shape of the dielectron invariant mass spectrum from the signal for various ρ_T masses, M_{ρ_T}, is shown in Fig. 9. The apparent width, $\mathcal{W}$, of the resonance (which is dominated by the detector resolution) increases with the mass of the particle.

Similar plots for acceptance, efficiency and signal shapes for the $Z' \to e^+e^-$ decays are shown in Figs. 7, 8 and 10, respectively.

TABLE II. Acceptance $\times$ efficiency for ρ_T or ω_T signals.

M_{ω_T} (GeV)	acc $\times$ eff
140	0.3060$\pm$0.0048
150	0.3103$\pm$0.0049
160	0.3207$\pm$0.0050
170	0.3283$\pm$0.0051
180	0.3384$\pm$0.0053
190	0.3374$\pm$0.0053
200	0.3396$\pm$0.0053
210	0.3434$\pm$0.0054
220	0.3527$\pm$0.0055
230	0.3545$\pm$0.0055
240	0.3560$\pm$0.0056
250	0.3631$\pm$0.0057
260	0.3606$\pm$0.0057
270	0.3666$\pm$0.0058
300	0.3735$\pm$0.0059
350	0.3828$\pm$0.0062
400	0.3974$\pm$0.0065
450	0.3976$\pm$0.0066

IV. LIMIT CALCULATION

In the absence of a signal above background, we proceed to set an upper limit on the cross section times branching fraction as a function of dielectron invariant mass. The limit is computed by fitting to the shape of the entire spectrum.

We calculate the limit in a way similar to that described in Ref. [3]. For each bin i in Figs. 1 and 3, we numerically calculate the probability $p(n_i|\mu_i)$ to observe the number of events seen n_i, given the expected number μ_i. In the calculation, we take into account the uncertainties in the value of μ_i:

$$\begin{aligned}\mu_i = {} & f_i \times \sigma \times \epsilon \times \mathcal{L} \\ & + b_i^1 \times (1 + \delta b_i^{sys} \times \mathcal{G}) \times (1 + \delta b_i^{stat} \times \mathcal{G}) \\ & + b_i^2 \times (1 + \delta b^2 \times \mathcal{G}) \times \mathcal{L},\end{aligned} \tag{2}$$

where $\mathcal{L} = \mathcal{L}_0(1 + \delta\mathcal{L} \times \mathcal{G})$ and $\epsilon = \epsilon_0(1 + \delta\epsilon \times \mathcal{G})$. The symbol $\mathcal{G}$ represents a random number from a Gaussian distribution with zero mean and unit width. All parameters with subscript i can differ from bin to bin. All other parameters have a single value, independent of bin. The parameters are:

- f_i – fraction of signal events in bin i;

- σ – signal cross section;
- ϵ_0 – estimate of signal efficiency;
- $\delta\epsilon$ – relative uncertainty in ϵ_0;
- $\mathcal{L}_0$ – estimate of integrated luminosity;
- $\delta\mathcal{L}$ – relative uncertainty in $\mathcal{L}_0$;
- b_i^1 – number of QCD background events expected in bin i;
- δb_i^{sys} – relative systematic error in b_i^1;
- δb_i^{stat} – relative statistical error in b_i^1;
- b_i^2 – expected cross section of Drell-Yan background in bin i;
- δb^2 – relative uncertainty in b_i^2.

The logarithm of the probability $p_i = p(n_i|\mu_i)$ is given by

$$\ln p_i = -\mu_i + n_i \ln \mu_i - \Gamma(n_i + 1) \tag{3}$$

We average this value over many throws of the random numbers $\mathcal{G}$ to reduce statistical fluctuations. The averaged logarithm of the joint probability for all bins is given by $\ln P = \langle \sum_i \ln p_i \rangle$. We calculate the corresponding values for the CC/CC data sample ($\ln P_{CC}$) and for the CC/EC data sample ($\ln P_{EC}$).

We determine the 95% confidence level upper limit on the signal cross section (σ_{95}) from the definition

$$\frac{\int_0^{\sigma_{95}} P_{CC}(\sigma) * P_{EC}(\sigma) d\sigma}{\int_0^{\infty} P_{CC}(\sigma) * P_{EC}(\sigma) d\sigma} = 0.95. \tag{4}$$

The result is shown in Fig. 11.

V. LIMITS ON TECHNICOLOR PARTICLES

Recent topcolor-assisted technicolor models with walking gauge coupling require many technihadron states. These models predict the existence of scalar mesons, the technipions ($\pi_T^{\pm}$ and π_T^0), and vector mesons (ρ_T and ω_T). These technihadron states are expected to be produced with substantial rates at the Tevatron [4]. The vector mesons decay to $\gamma\pi_T$, $W\pi_T$, $Z\pi_T$, or fermion-antifermion pairs. No large isospin violating technicolor interactions are needed to explain the mass difference between the top and bottom quarks. Therefore, the ρ_T and ω_T states can be (and are assumed to be) degenerate in mass. As shown in Ref. [5], most of the rate to dilepton final states originates from ω_T decays, so that our conclusions for the mass of the ω_T do not depend strongly on this assumption.

The values of $\sigma(\rho_T, \omega_T) \times B(\rho_T, \omega_T \to \ell\ell)$ depend on the following factors:

TABLE III. Cross sections for dielectron production in $p\overline{p}$ collisions via ω_T and ρ_T. All mass values in GeV.

M_{ω_T}		cross section × branching fraction (fb)				
(GeV)	$M_{\rho_T} - M_{\pi_T}$	60	100	100	100	100
	M_T	100	100	200	300	400
150		1100	730	880	950	980
180		500	310	380	420	430
220		230	140	200	230	250
250		140	810	120	140	160
300		69	38	60	73	79
350		36	19	32	39	42
400		20	10	18	21	23
450		11	6	10	12	13

- mass of ρ_T (M_{ρ_T}) and ω_T (M_{ω_T})
- mass difference between the vector mesons (ρ_T, ω_T) and the technipions, which determines the spectrum of accessible decay channels.

In addition, the ω_T production cross section is sensitive to the charges of the technifermions, as well as to a mass parameter [1] M_T that controls the rate for $\omega_T \to \gamma + \pi_T^0$. This mass parameter is unknown *a priori*. Scaling from the decay $\omega \to \gamma + \pi^0$ the authors suggest a value of several 100 GeV. For all other parameters, we use the default values quoted in Table 2 of Ref. [6].

We use recently updated calculations of the cross sections for $p\overline{p} \to \rho_T \to \ell^+\ell^-$ and $p\overline{p} \to \omega_T \to \ell^+\ell^-$ [5,6]. Previously published searches for technicolor particles [7] use older calculations. When comparing limits this must be taken into account. The predictions for the cross sections of the processes $p\overline{p} \to (\rho_T \text{ or } \omega_T) \to e^+e^-$ are tabulated in Table III and plotted in Fig. 11. In this figure, the two predictions shown differ in the assumed mass difference between the vector and scalar mesons. For a mass difference smaller than the mass of the W boson (e.g., 60 GeV), the decay $\rho_T \to W + \pi_T$ is forbidden and the branching ratio to dielectrons is enhanced compared to the case of a mass difference of 100 GeV, for which the $W\pi_T$ mode is allowed.

We find that we can rule out ρ_T and ω_T with masses below 207 GeV, if the mass difference between ρ_T and $\pi_T^\pm$ is smaller than the W mass.

The limit depends on the choice of the parameter M_T, as illustrated in Fig. 12. In this figure the experimental limit is compared to predictions in which the parameter M_T, which

[1]In Ref. [5], two parameters, M_A for axial-vector and M_V for vector couplings, appear. Their values are expected to be comparable. We set $M_A = M_V = M_T$.

TABLE IV. K-factor used for Z' search.

Mass Range	Cross Section (*10^{-3}pb)	K-Factor
300	3124	1.336
400	907.1	1.381
500	286.9	1.431
600	95.4	1.483
700	31.9	1.532
800	10.1	1.568
900	3.75	1.608

controls the ω_T cross section, is varied. For example, for values of $M_T > 200$ GeV we can rule out ρ_T and ω_T with masses below 203 GeV.

VI. LIMIT ON A HEAVY NEUTRAL GAUGE BOSON

There are no unique predictions for the couplings of a heavy neutral gauge boson (Z') to fermions. Thus we assume as a benchmark the couplings of the standard model Z boson, adjusted for the higher mass. We determine the cross section times branching ratio using PYTHIA and adjust for the K-factor listed in Table IV. This K-factor was determined for a previous Z' search by the DØ Collaboration in a smaller data set [8].

We set the limit using the same algorithm as for the technicolor particles. Figure 13 shows the experimental limit together with the theoretical cross section. For the assumed couplings, we exclude the existence of a Z' below a mass of 670 GeV at 95% confidence level. The previous search by DØ [8] using a smaller data sample set a limit at 490 GeV. A search by CDF [9] set a limit at 690 GeV.

VII. CONCLUSION

Based on 120.9 pb^{-1} of data collected by the DØ detector at the Tevatron during 1992-1996, we set limits on the production of technirho (ρ_T), techniomega (ω_T), and Z' particles in $p\overline{p}$ collisions using their decay to e^+e^- . The 95% CL upper limits on the particle masses are 207 GeV for ρ_T and ω_T states, assuming that they have equal mass and that the decay $\rho_T \rightarrow \pi_T + W$ is not allowed, and 670 GeV for Z' bosons with standard model couplings.

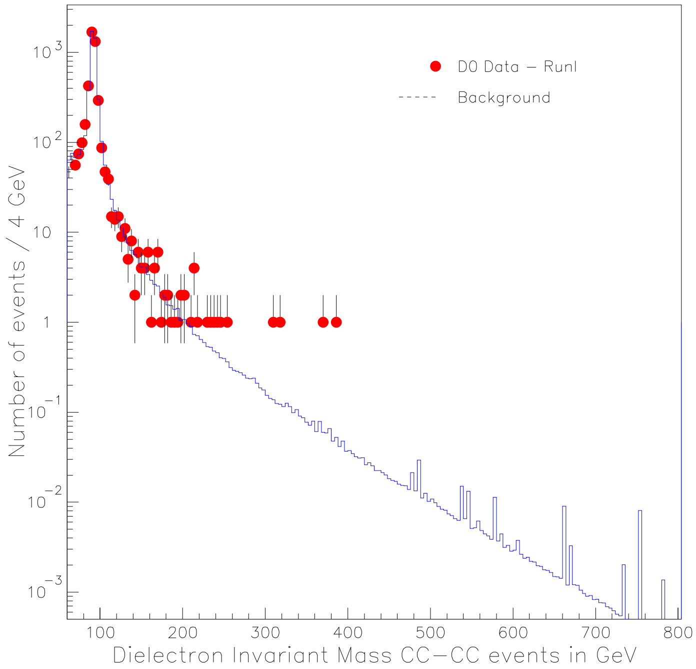

FIG. 1. Dielectron invariant mass spectrum for CC/CC events.

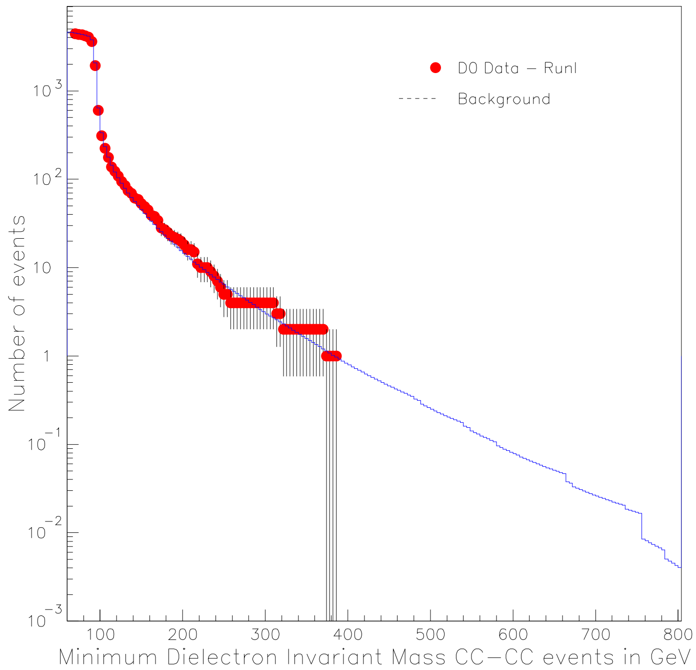

FIG. 2. Integrated dielectron invariant mass spectrum for CC/CC events.

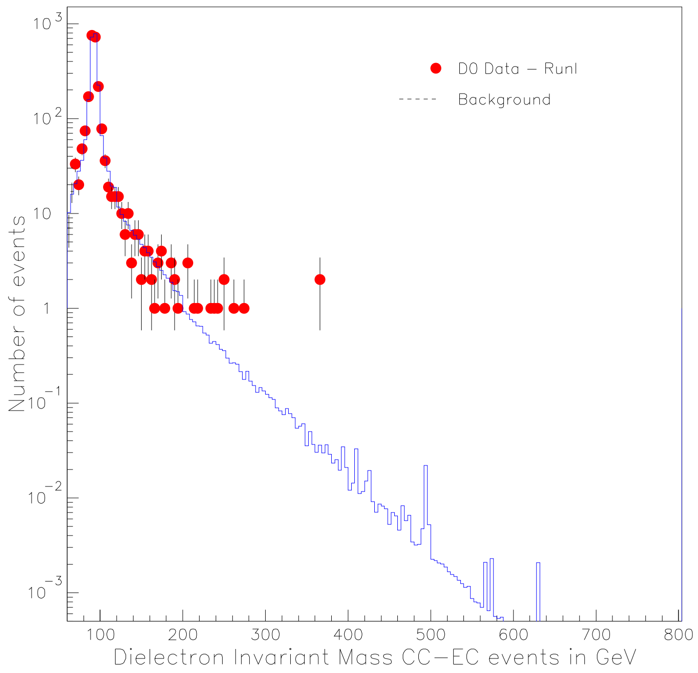

FIG. 3. Dielectron invariant mass spectrum for CC/EC events.

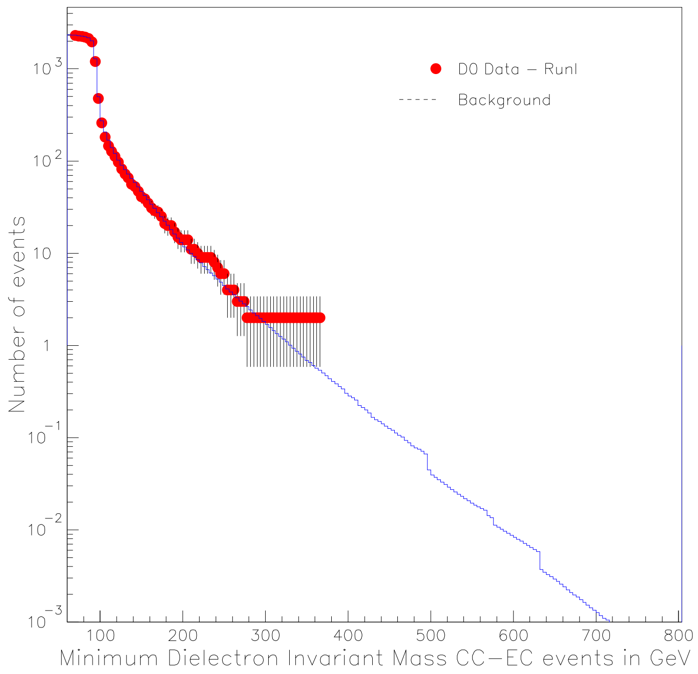

FIG. 4. Integrated dielectron invariant mass spectrum for CC/EC events.

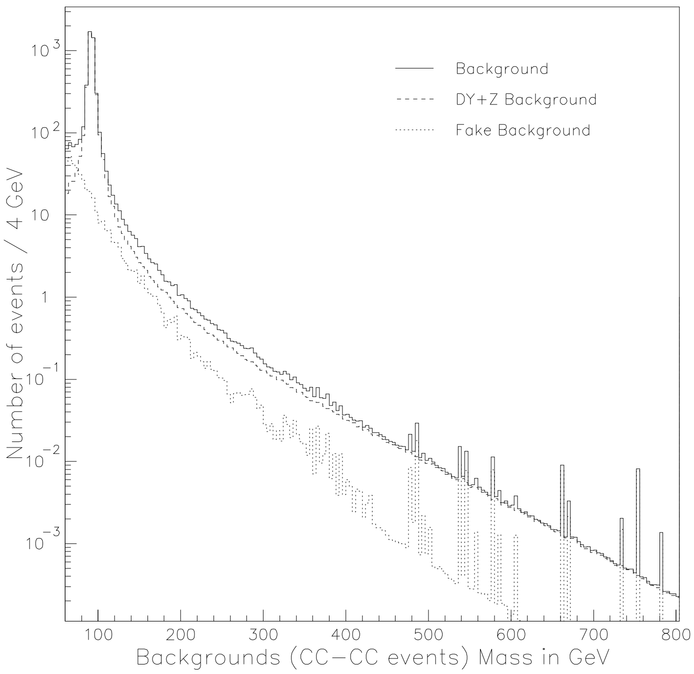

FIG. 5. Dielectron invariant mass for CC/CC backgrounds.

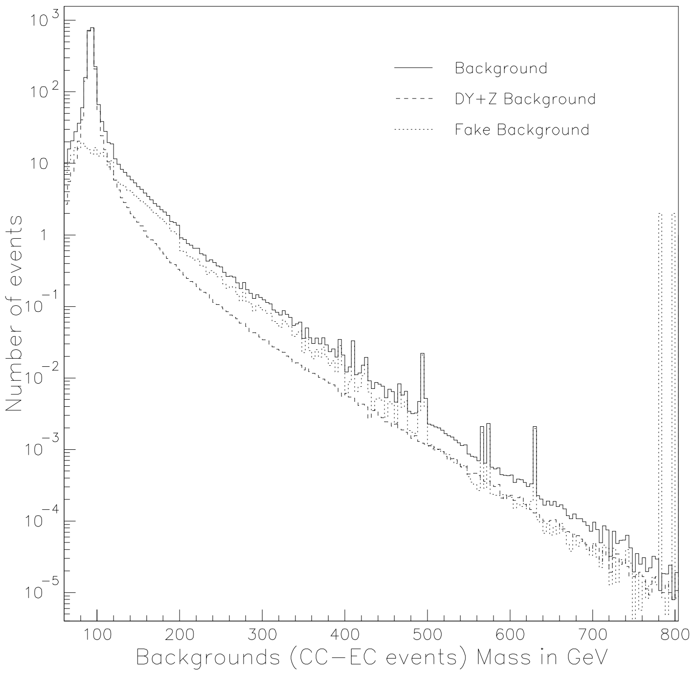

FIG. 6. Dielectron invariant mass for CC/EC backgrounds.

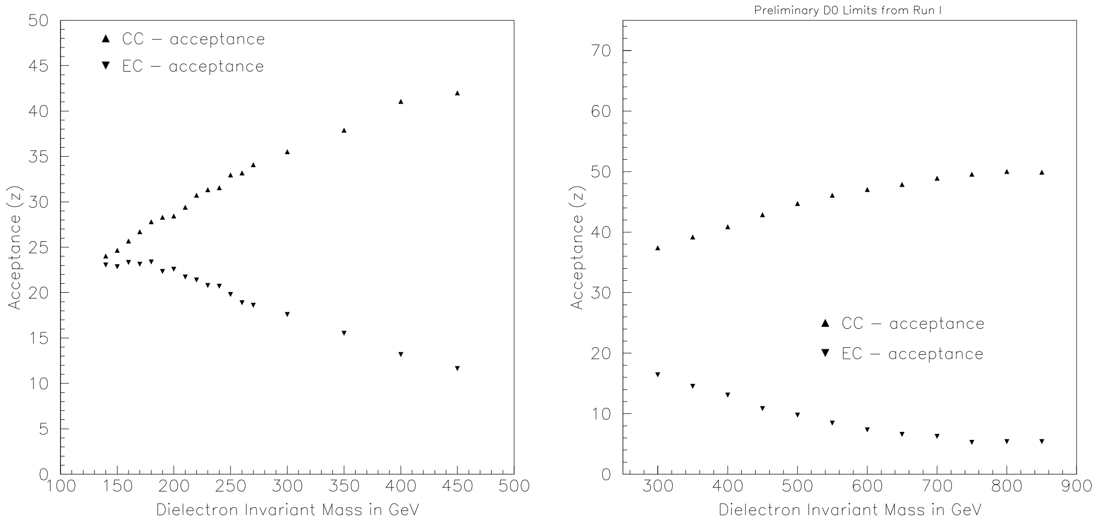

FIG. 7. Acceptance for $\rho_T, \omega_T \to e^+e^-$ events (left) and for $Z' \to e^+e^-$ events (right).

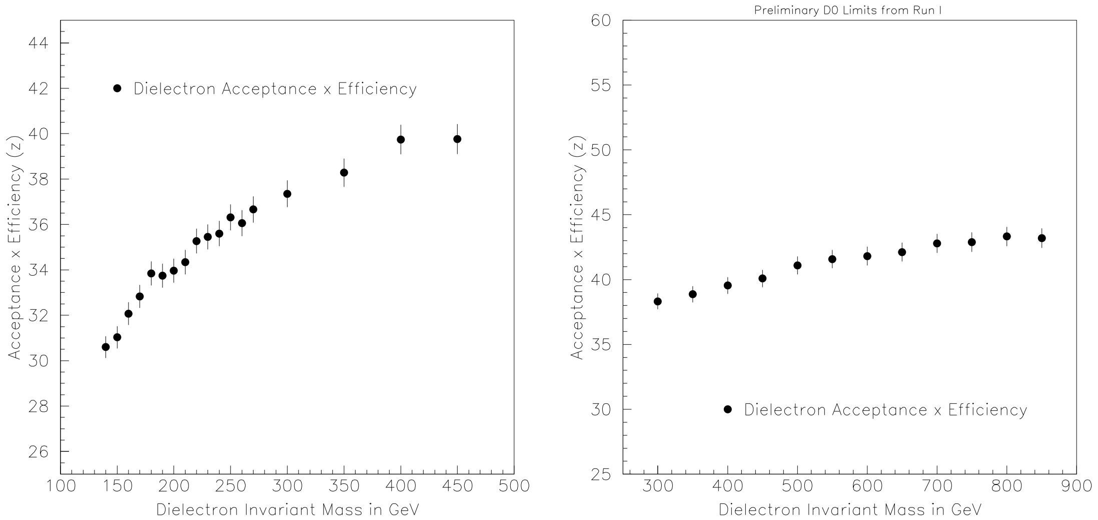

FIG. 8. Efficiency for detecting $\rho_T, \omega_T \to e^+e^-$ events (left) and $Z' \to e^+e^-$ events (right).

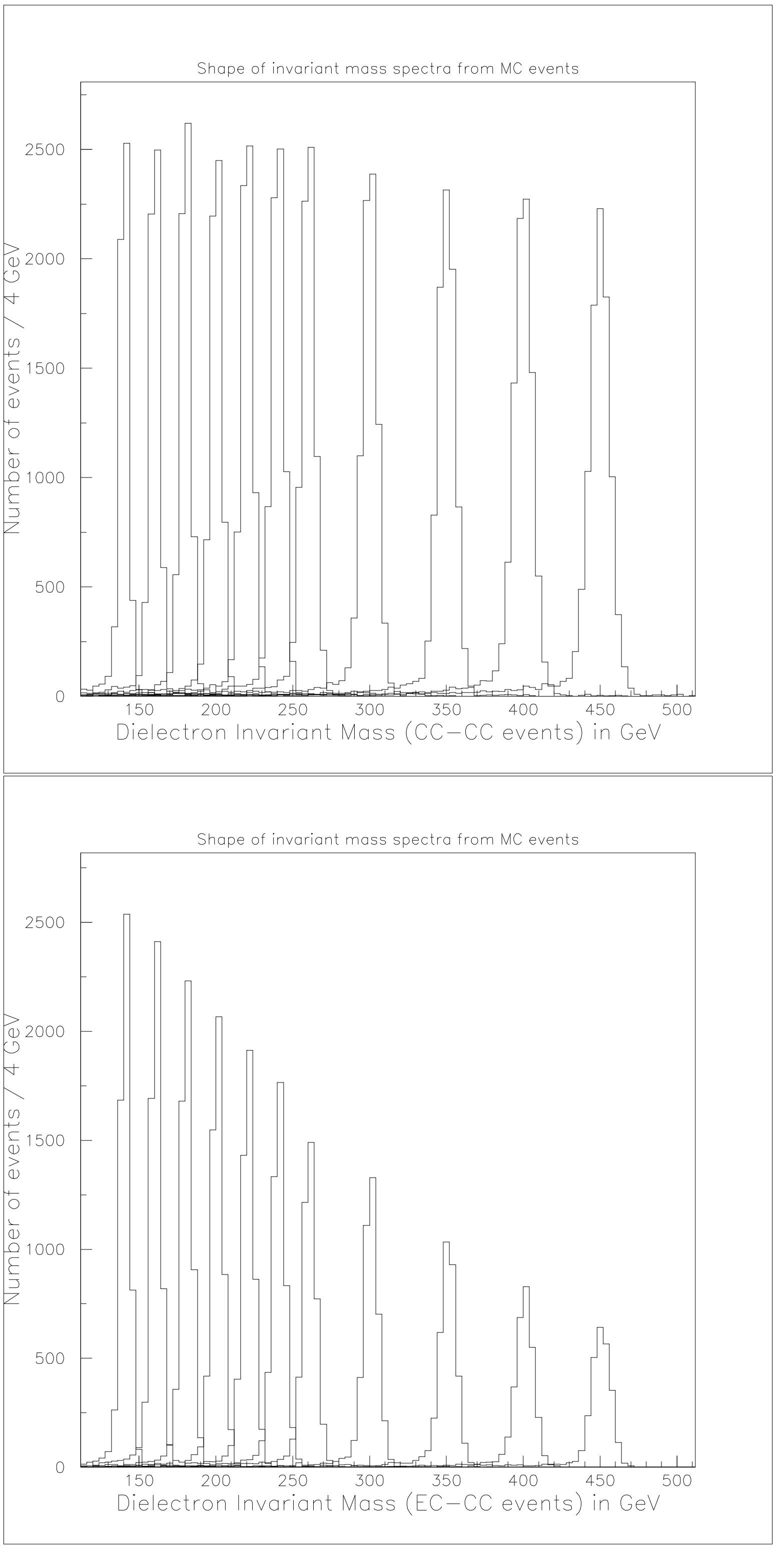

FIG. 9. Shapes of the dielectron invariant mass spectra for the $\rho_T, \omega_T \to e^+e^-$ signal.

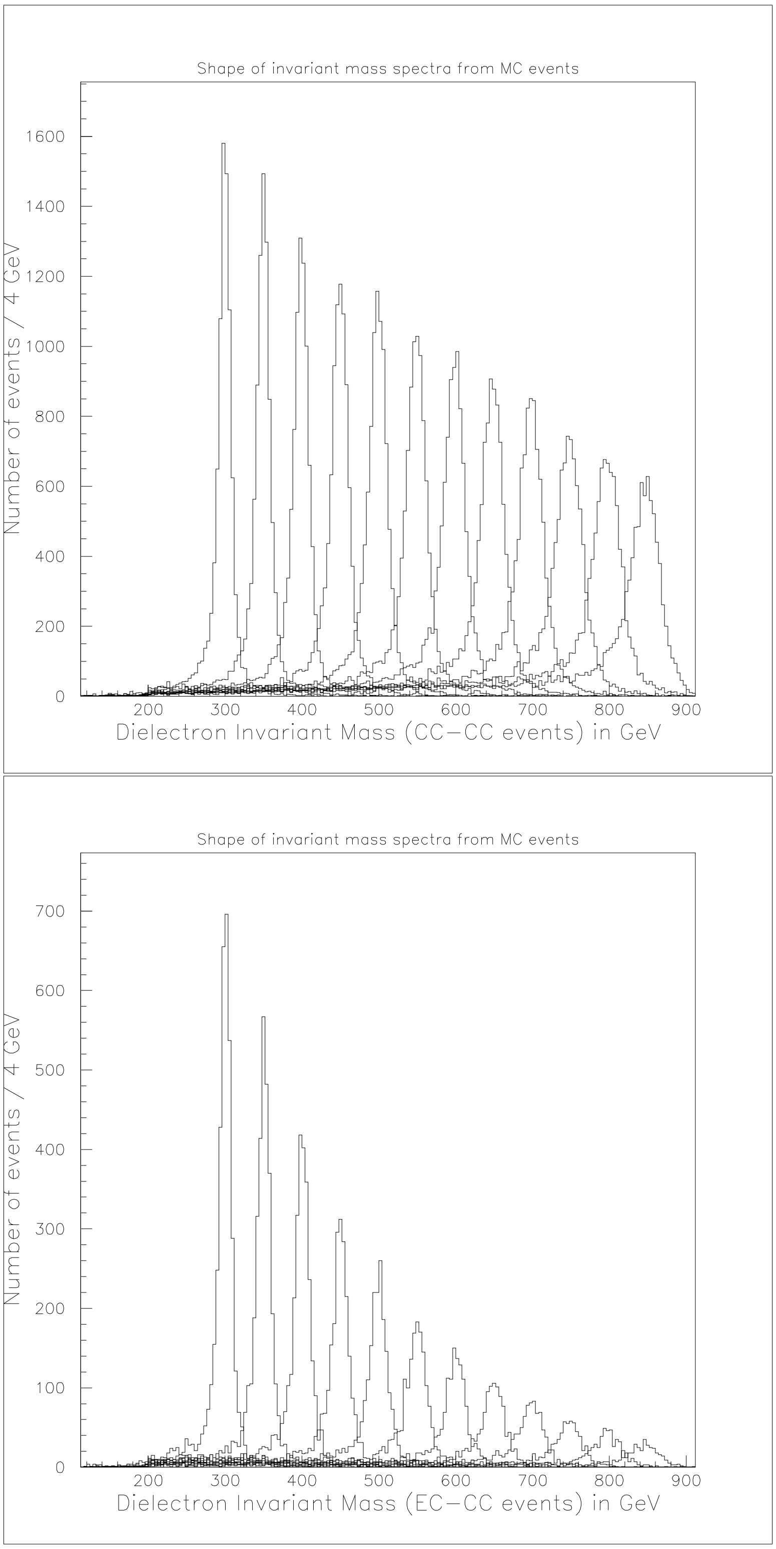

FIG. 10. Shapes of the dielectron invariant mass spectra for the $Z' \to e^+e^-$ signal.

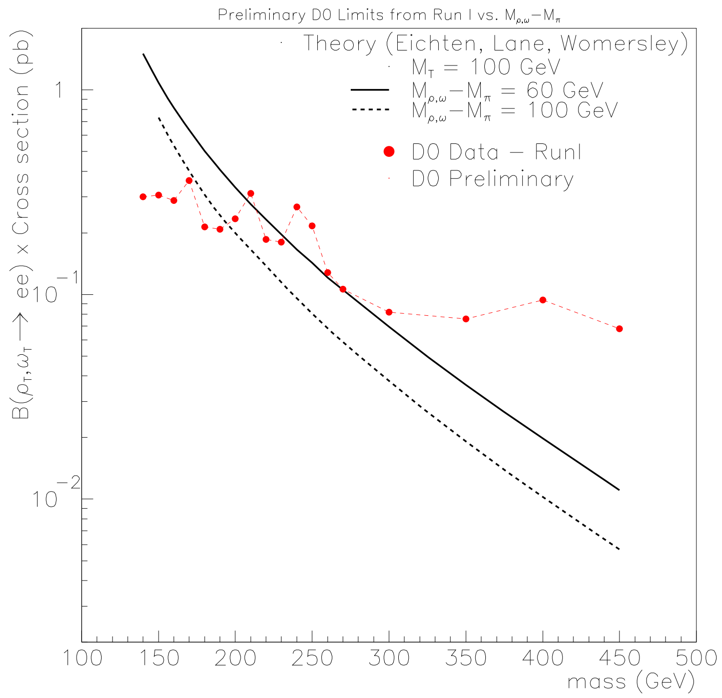

FIG. 11. Experimental upper limits at 95% confidence level for $\rho_T, \omega_T \to e^+e^-$ production compared with predictions.

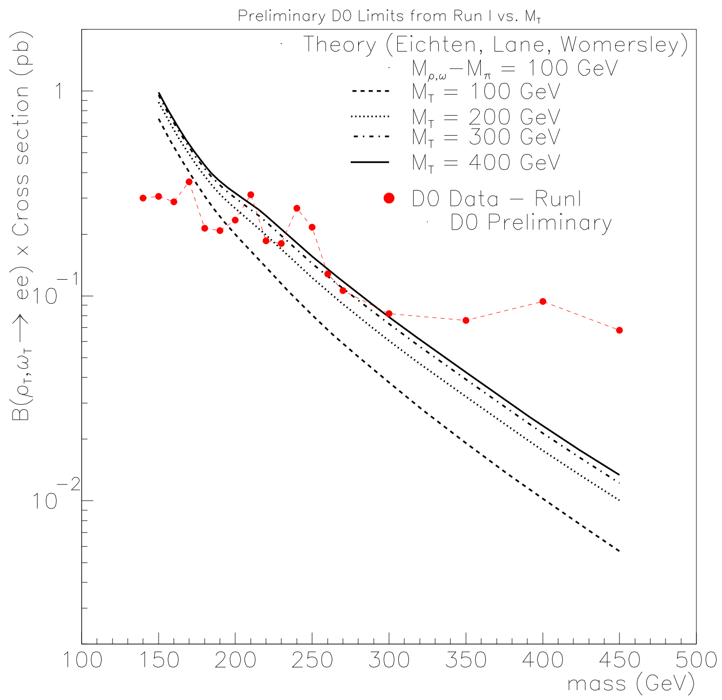

FIG. 12. Experimental upper limits at 95% confidence level for $\rho_T, \omega_T \to e^+e^-$ production compared with predictions.

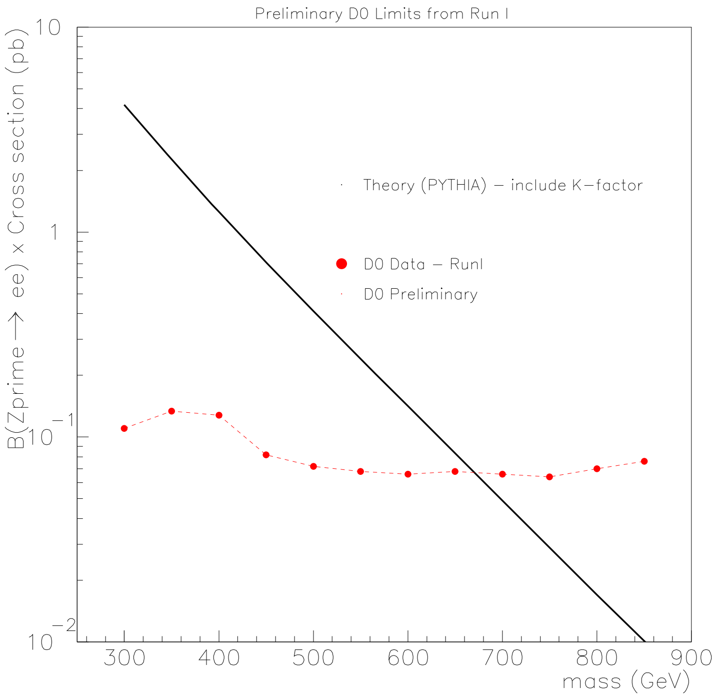

FIG. 13. Experimental upper limit at 95% confidence level for $Z' \to e^+e^-$ production compared with predictions.

ACKNOWLEDGEMENTS

We thank Ken Lane for helpful discussions at the Aspen Center for physics, where this analysis was started. We also acknowledge the support of the Aspen Center for Physics. We thank the staffs at Fermilab and at collaborating institutions for contributions to this work, and acknowledge support from the Department of Energy and National Science Foundation (USA), Commissariat à L'Energie Atomique and CNRS/Institut National de Physique Nucléaire et de Physique des Particules (France), Ministry for Science and Technology and Ministry for Atomic Energy (Russia), CAPES and CNPq (Brazil), Departments of Atomic Energy and Science and Education (India), Colciencias (Colombia), CONACyT (Mexico), Ministry of Education and KOSEF (Korea), CONICET and UBACyT (Argentina), A.P. Sloan Foundation, and the Humboldt Foundation.

REFERENCES

[1] DØ Collaboration, Phys. Rev. Letters **82**, 4769 (1999).

[2] PYTHIA

[3] DØ Collaboration, Phys. Rev. Letters **82**, 2457 (1999).

[4] E. Eichten, K. Lane and J. Womersley, Phys. Lett. **B405**, 305-311 (1997).

[5] K. Lane, "Technihadron production and decay in low-scale technicolor", hep-ph/9903369.

[6] K. Lane, "Technihadron production and decay rates in the technicolor straw man model", hep-ph/9903372.

[7] CDF Collaboration, FERMILAB-PUB-99/141-E, submitted to Phys. Rev. Letters.

[8] DØ Collaboration, Phys. Lett. **B385**, 471 (1996).

[9] CDF Collaboration, FERMILAB-PUB-97/122-E, submitted to Phys. Rev. Letters.